RESEARCH ARTICLE

A global climate model ensemble for downscaled monthly climate normals over North America

Colin R. Mahony[1] | Tongli Wang[2] | Andreas Hamann[3] | Alex J. Cannon[4]

[1]British Columbia Ministry of Forests, Lands, Natural Resource Operations and Rural Development, Victoria, British Columbia, Canada

[2]Centre for Forest Conservation Genetics, Department of Forest and Conservation Sciences, Faculty of Forestry, University of British Columbia, Vancouver, British Columbia, Canada

[3]Department of Renewable Resources, Faculty of Agricultural, Life, and Environmental Sciences, University of Alberta, Edmonton, Alberta, Canada

[4]Climate Research Division, Environment and Climate Change Canada, Victoria, British Columbia, Canada

Correspondence
Colin R. Mahony, British Columbia Ministry of Forests, Lands, Natural Resource Operations and Rural Development, Victoria, BC, Canada.
Email: colin.mahony@gov.bc.ca

Abstract

Use of downscaled global climate model projections is expanding rapidly as climate change vulnerability assessments and adaptation planning become mainstream in many sectors. Many climate change impact analyses use climate model projections downscaled at very high spatial resolution (~1 km) but very low temporal resolution (20- to 30-year normals). These applications have model selection priorities that are distinct from analyses at high temporal resolution. Here, we select a 13-model ensemble and an 8-model subset designed for robust change-factor downscaling of monthly climate normals, and describe their attributes in North America. All models are selected from the Coupled Model Intercomparison Project Phase 6 (CMIP6) archives. The 13-model ensemble is representative of the distribution of equilibrium climate sensitivity, grid resolution, and transient regional climate changes in the CMIP6 generation. The 8-model subset is consistent with the IPCC's recent assessment of the *very likely* range of Earth's equilibrium climate sensitivity. Our results emphasize several principles for selection and use of downscaled climate ensembles: (a) the ensemble must be observationally constrained to be meaningful; (b) analysis of multiple models is essential as the ensemble mean alone can be misleading; (c) small (<8-member) ensembles should be region-specific and used with caution; (d) higher grid resolution is not necessarily better; and (e) multiple simulations of each model/scenario combination are necessary to represent precipitation uncertainty. Although we have focused our documentation on North America, our model selection uses primarily global criteria and is applicable to downscaling climate normals in other continents. Downscaled projections for the selected models are available in ClimateNA (http://climatena.ca/). An accompanying web application (https://bcgov-env.shinyapps.io/cmip6-NA/) provides tools for further model selection and visualization of the ensemble.

KEYWORDS
climate change, CMIP6, downscaling, ensembles, North America

1 | INTRODUCTION

The Sixth iteration of the Coupled Model Inter-comparison Project (CMIP6; Eyring *et al.*, 2016) is a once-in-a-decade update to projections of climate change. CMIP6 provides a larger number of simulations from a new generation of global climate models, at higher spatial resolution, and using an improved set of emissions scenarios relative to its predecessor, CMIP5 (Taylor *et al.*, 2012). These new climate simulations contribute to and are put into broader context by the Sixth Assessment Report from Working Group I of the Intergovernmental Panel on Climate Change (Lee *et al.*, 2021). CMIP6 simulations are rapidly being incorporated into downscaled climate data products for use in regional climate change impacts and adaptation initiatives. These initiatives can benefit from careful selection of climate model projections that are suited to broad classes of end uses (e.g., Karmalkar *et al.*, 2019), and their wide application requires transparency on the attributes of these ensembles.

Many climate change impact analyses, particularly in ecology, use projections of climate change that are downscaled to very high resolution (~1 km) but very low temporal resolution (20- to 30-year climate normals). The prevalence of this type of analysis is evident from the widespread use of WorldClim (Hijmans *et al.*, 2005; Fick and Hijmans, 2017; 23,340 citations) and ClimateNA (Wang *et al.*, 2012; 2016; Hamann *et al.*, 2013; 1,678 citations). The low temporal resolution of these applications simplifies downscaling; both WorldClim and ClimateNA use change-factor downscaling, also called the climate imprint method (Hunter and Meentemeyer, 2005) and simple mean bias correction (Maraun, 2016). This method adds low-spatial-resolution anomalies from the climate model to a high-resolution gridded climate map (Tabor and Williams, 2010). The best practices for change-factor downscaling to high-spatial and low-temporal resolution are different than those for the more sophisticated statistical downscaling techniques necessary for high temporal resolution downscaling (Wilby *et al.*, 2004), leading to distinct model selection priorities.

One consideration in model selection for change-factor downscaling is the number of simulation runs for each candidate model. The change-factor method is sensitive to the influence of natural variability in the historical reference period against which anomalies are calculated and bias correction is applied. Performing change-factor downscaling with multiple simulation runs of each model reduces the confounding influence of natural variability in bias correction and improves the signal-to-noise ratio (Milinski *et al.*, 2019). Further, providing multiple simulations for each model and scenario can improve the representation of climate change uncertainty in downstream analysis by accounting for natural variability (Deser *et al.*, 2012). Consequently, models with multiple simulations for the historical period and each future scenario are preferable in this context.

Another consideration is model bias. All climate models exhibit biases—systematic differences between observations and simulations—at the regional scale. Removal of these biases is a basic step in downscaling (Maraun, 2016). Change-factor downscaling performs univariate bias correction and therefore may not conserve the physical (e.g., thermodynamic) interdependence between variables such as temperature and precipitation (Cannon, 2018). The associated potential for univariate downscaling to produce physically implausible climatic conditions presumably increases with the size of the biases in the simulation. For this reason, models with small biases are preferable to models with large biases, all else being equal.

Finally, the spatial resolution of climate models is of interest to high spatial resolution downscaling. Some models contributing to the CMIP6 ScenarioMIP (O'Neill *et al.*, 2016) experiment (the candidate pool for ensemble selection in this study) have horizontal grid resolutions of 70–100 km. These higher-resolution models are able to resolve macrotopography, for example, to differentiate the major mountain ranges within the Western Cordillera. The opportunity to better represent the influences of water bodies and topography on climate change trends, such as elevation-dependent warming (Salathé *et al.*, 2008; Palazzi *et al.*, 2019), is appealing for climate change impact analyses. Conversely, models with very low spatial resolution (>300 km) can conflate the climate change signals of distinct regions, particularly at land/ocean transitions (Lanzante *et al.*, 2018). Very low resolution therefore is a consideration for exclusion from ensembles designed for high-resolution change-factor downscaling.

Collectively, the three considerations described above suggest an ensemble that prioritizes number of simulations per model rather than number of models, low-to-moderate bias, and moderate-to-high spatial resolution.

Once a general-purpose ensemble is selected, it is useful to structure the ensemble for further user-specific model selection. Many applications of projected climate normals are computationally intensive analyses at regional scales. In these cases, it can be desirable to use a small number (3–8) of models that represent the approximate range of a more comprehensive ensemble. Cannon (2015) describes a method for structuring an ensemble into an order of subset selection that optimally represents the ensemble spread. Alternatively, analysts may wish to select a custom subset of the ensemble.

Documentation of the attributes of the ensemble members can help analysts to identify subsets that are best suited to specific applications.

The purpose of this study is to select and describe an ensemble of CMIP6 model projections of 21st century climate change over North America. The focus of model selection is on facilitating robust downscaling of projected climate normals at very high spatial resolution. We characterize the attributes, biases, and climate change trends of the ensemble and highlight features of interest in individual climate models. We further screen this selected ensemble to an 8-model subset consistent with IPCC assessed constraints on equilibrium climate sensitivity (Arias *et al.*, 2021). Finally, we provide a selection order for the 8-model subset for regional analyses. Downscaled projections for the selected 13 CMIP6 models are available in ClimateNA (http://climatena.ca/), which provides downscaling at user-specified spatial resolution and various temporal intervals (annual, 20-year, and 30-year periods). An accompanying web application (https://bcgov-env.shinyapps.io/cmip6-NA/) provides tools for further model selection and visualization of the ensemble.

2 | METHODS

2.1 | Criteria for model selection

We assessed all models in the Earth System Grid Federation (ESGF) archive for the CMIP6 ScenarioMIP as of December 15, 2020. We selected models using six objective criteria, listed below with rationale:

- Criterion 1: T_{min} and T_{max} available. Mean daily minimum temperature (T_{min}) and mean daily maximum temperature (T_{max}) are the directly measured elements of the long-term temperature record, and are the fundamental temperature elements in many climate change impact analyses.
- Criterion 2: Minimum of three historical runs available. This criterion ensures robust downscaling by reducing the confounding influence of natural variability in bias correction.
- Criterion 3: Complete scenarios. Models need to have at least one simulation for three of the four major shared socioeconomic pathways (SSP) marker scenarios (SSP1-2.6, SSP2-4.5, SSP3-7.0, and SSP5-8.5).
- Criterion 4: One model per institution. This criterion is a widely applied best practice in ensemble selection (Leduc *et al.*, 2016) as one measure to increase independence among ensemble members. For the purposes of this criterion, different physics or forcing

schemes of the same model were considered different models.
- Criterion 5: No closely related models. Models that share components were excluded, following Brunner *et al.* (2020, fig. 5).
- Criterion 6: No large biases. Bias is the degree to which a model simulation differs from the observed climate over a historical reference period). Models with large biases relative to the rest of the ensemble in one or more variables were excluded.

2.2 | Ensemble subset criteria

Users of the ensemble may wish or need to use a lesser number of models in their analyses. To support the selection of subsets, we structure the ensemble by defining an order of exclusion of models. Models are excluded in two phases: first based on screening criteria and second using the method of Cannon (2015) to represent the range of climate changes in the remaining models.

2.2.1 | Screening criteria

Priority for exclusion from model subsets was established using four screening criteria. The screening criteria are more subjective than the six selection criteria defined above. They generally are not sufficient in isolation but combinations of the criteria provide some justification for model exclusions.

- Criterion 7: Constraints on equilibrium climate sensitivity (ECS). Multiple lines of evidence indicate that the Earth's ECS is *likely* (probability >66%) between 2.5 and 4°C and *very likely* ($p > 90\%$) between 2 and 5°C (Sherwood *et al.*, 2020; Arias *et al.*, 2021). The evidence is robust for the lower bound, and weaker for the upper bound. From one perspective, inclusion of models with ECS outside this *very likely* range biases the multimodel ensemble mean and unnecessarily increases the modelling uncertainty in downstream analyses (Ribes *et al.*, 2021). An alternate perspective is that high-sensitivity models are useful as a representation of high-impact, low-likelihood scenarios (Sutton and Hawkins, 2020). To accommodate both perspectives, we provide structured subsets with and without high-sensitivity models.
- Criterion 8: Model resolution. Some ScenarioMIP models have sufficiently high spatial resolution to resolve macrotopography, for example, to differentiate the major mountain ranges of the Western Cordillera. These models are weighted towards inclusion from the

ordered subsets. Models with very low spatial resolution are weighted towards exclusion from the subsets.

- Criterion 9: Number of simulation runs. Models with only one run per emissions scenario are weighted for exclusion.
- Criterion 10: Grid cell artefacts. Models exhibiting spatially anomalous climate changes in individual grid cells are problematic for many of the intended uses of this ensemble, and are weighted for exclusion from the ordered subsets.

2.2.2 | Ordered subsets

After exclusion of models using the screening criteria above, an order of exclusion for the remaining models is defined using the Katsavounidis–Kuo–Zhang (KKZ) algorithm, using the application to climate model ensemble selection described by Cannon (2015). KKZ deterministically selects models that best represent the spread of multivariate climate changes projected by the ensemble. KKZ subset selection is ordered, starting with the model closest to the ensemble centroid, and incrementally adding models to a region of the ensemble variation that is poorly represented by each successive subset.

Since the spatial patterns of climate change differ among models, we provide separate KKZ subsets for each of the seven IPCC climate reference regions (Iturbide et al., 2020) within North America. We also provide an ordered subset for North America as a whole, but caution that ensembles of less than eight models are likely insufficient to represent spatial variation in modelling uncertainty at continental scales (Pierce et al., 2009; McSweeney et al., 2014; Cannon, 2015). The implementation of KKZ in this study used the mean of the z-standardized seasonal changes in T_{min}, T_{max}, and precipitation in three consecutive 20-year time periods starting with 2041–2060 and two emissions scenarios (SSP2-4.5 and SSP3-7.0).

2.3 | Representation of the full CMIP6 ensemble

We use the ECS of the CMIP6 models (Meehl et al., 2020) as a basic assessment of whether the selected ensemble is globally representative of the full CMIP6 ensemble. However, matching the CMIP6 ensemble ECS does not guarantee that the selected ensemble is representative of transient temperature and precipitation changes at regional scales (Karmalkar, 2018). We compare transient climate change in the selected ensemble to 33 CMIP6

models for which we were able to obtain mean monthly temperature (tas) and precipitation (Table 1). Transient climate changes are calculated as the mean 2061–2100 SSP2-4.5 climate for each model simulation relative to the grand mean 1961–1990 climate of multiple historical simulations for each model. After visually identifying and removing outliers, we measured representiveness as the simple ratio of the univariate ranges in seasonal temperature and precipitation changes spanned by the selected ensemble relative and the larger CMIP6 ensemble (following the approach of Karmalkar, 2018).

2.4 | Analysis of model bias

We assessed model biases against the ClimateNA composite of PRISM and WorldClim observed gridded climate normals for the 1961–1990 period (Wang et al., 2016). We measured model bias as the *mean absolute bias* over North America in each monthly climate variable (T_{min}, T_{max}, and precipitation). For each grid cell, i, the mean simulated 1961–1990 climate normal of the K historical model runs, f_{ik} is calculated as

$$\overline{f}_i = \frac{1}{K}\sum_{k=1}^{K} f_{ik}. \tag{1}$$

The absolute value of the difference between the simulated 1961–1990 normal, $\overline{f}_i$, and the observed 1961–1990 normal, o_i, aggregated onto the native model grid is calculated for each grid cell:

$$|e_i| = |\overline{f}_i - o_i|. \tag{2}$$

The mean absolute bias, $|e|$, over all N projected grid cells in North America is calculated as

$$|e| = \frac{1}{N}\sum_{i=1}^{N} |e_i|. \tag{3}$$

To equalize the area of grid cells, we projected absolute bias in the native model grid onto a Lambert Conformal Conic grid with 0.5° resolution prior to calculating this mean.

For precipitation variables, Equations (1) and (2) were performed on log-transformed normals. Subsequent to Equation (3), this log-transformation was reversed by taking the exponent of absolute bias. Doing so expresses absolute bias of precipitation as a factor of magnitude. For example, simulated precipitation normals of 50% and 200% relative to observed precipitation both have an absolute bias of 2.

TABLE 1 Candidate models, model exclusion criteria, and number of simulation runs

Model		Criterion for exclusion	ECS	ESGF holdings					Analysed				
				Historical	ssp126	ssp245	ssp370	ssp585	Historical	ssp126	ssp245	ssp370	ssp585
ACCESS-CM2	2	<3 historical runs	4.7	2	1	1	1	1					
ACCESS-ESM1-5			3.9	30	10	30	10	10	10	10	10	10	10
AWI-CM-1-1-MR	6	Very high bias	3.2	5	1	1	5	1					
BCC-CSM2-MR			3.3	3	1	1	1	1	3	1	1	1	1
CAMS-CSM1-0	1	No Tmax/Tmin	2.3	3	2	2	2	2					
CESM2	1	No Tmax/Tmin in historical	5.2	11	3	3	3	3					
CESM2-WACCM	1	No Tmax/Tmin in historical	4.8	3	1	5	3	5					
CIESM	3	Incomplete scenarios		3	1			1					
CMCC-CM2-SR5	1	No Tmax/Tmin		1	1	1	1	1					
CNRM-CM6-1	4	Same institution	4.9	30	6	10	6	6					
CNRM-CM6-1-HR	2	<3 historical runs	4.3	1	1	1	1	1					
CNRM-ESM2-1			4.8	11	5	10	5	5	11	5	5	5	5
CanESM5			5.6	65	50	50	50	50	10	10	10	10	10
CanESM5-CanOE	4	Same institution		3	3	3	3	3					
E3SM-1-1	3	Incomplete scenarios	5.3	1				1					
EC-Earth3			4.3	73	7	30	7	58	5	5	5	5	5
EC-Earth3-AerChem	2	<3 historical runs		2			1						
EC-Earth3-Veg	4	Same institution	4.3	8	7	8	6	6					
FGOALS-f3-L	1	No Tmax/Tmin	3	3	3	3	3	3					
FGOALS-g3	1	No Tmax/Tmin	2.9	6	4	4	5	4					
FIO-ESM-2-0	3	Incomplete scenarios		3	3	3		3					
GFDL-CM4	3	Incomplete scenarios	3.9	1	1	1	1	1					
GFDL-ESM4			2.7	3	1	3	1	1	3	1	3	1	1
GISS-E2-1-G		r*i1p3f1 variants	2.7	47	7	30	19	7	4	4	4	4	4
HadGEM3-GC31-LL	5	Shared components	5.6	5	1	4		4					
HadGEM3-GC31-MM	3	Incomplete scenarios	5.4	4	1		1	4					
IITM-ESM	1	No Tmax/Tmin		1	1	1	1	1					
INM-CM4-8	2	<3 historical runs	1.8	1	1	1	1	1					
INM-CM5-0			1.9	9	1	1	5	1	9	1	1	5	1
IPSL-CM6A-LR			4.6	9	5	6	9	5	9	5	6	9	5

(Continues)

TABLE 1 (Continued)

Model	Criterion for exclusion	ECS	ESGF holdings					Analysed				
			Historical	ssp126	ssp245	ssp370	ssp585	Historical	ssp126	ssp245	ssp370	ssp585
KACE-1-0-G	1 No Tmax/Tmin		3	3	3	3	3	3		3		
KIOST-ESM	2 <3 historical runs		1	1	1		1					
MCM-UA-1-0	1 No Tmax/Tmin		2	1	1	1	1	1		1		
MIROC-ES2L	4 Same institution	2.7	3	3	3	3	3	3	3	3		
MIROC6		**2.6**	50	50	50	3	50	10	10	10	3	10
MPI-ESM-1-2-HAM	3 Incomplete scenarios		3			2						
MPI-ESM1-2-HR		**3**	10	2	2	10	2	8	2	2	10	1
MPI-ESM1-2-LR	4 Same institution	3	10	10	10	10	10	10	10	10		
MRI-ESM2-0		**3.1**	7	1	5	5	2	5	1	5	1	1
NESM3	5 Shared components	4.8	5	2	2		2	5	2	2		
NorESM2-LM	1 No Tmax/Tmin	2.6	3	1	3	3	1	3	3	3		
NorESM2-MM	1 No Tmax/Tmin	2.5	1	1	2	1	1	1		1		
TaiESM1	1 No Tmax/Tmin	4.4	2	1	1	1	1					
UKESM1-0-LL		**5.4**	19	16	17	16	5	10	5	5	5	5

Note: Grey shading indicates models evaluated for bias. Bold font indicates the 13 models that passed Criteria 1–6. Model list and number of simulations per scenario are ESGF holdings as of December 15, 2020. ECS is equilibrium climate sensitivity (long-term temperature change in response to an instant doubling of CO_2); ECS values are quoted from Meehl *et al.* (2020), supplemented by Schlund *et al.* (2020). See Table 2 for citations and institutions of selected models.

2.5 | Cluster analysis

For visualization of similarity among models, we perform a cluster analysis on six climate variables—T_{min}, T_{max}, and precipitation for winter (DJF) and summer (JJA)—at 325 locations by resampling all models to a common 300 km resolution. To reduce dimensions for clustering, we used three principal components instead of the original six variables, resulting in 975 variables for the construction of the dendrogram (325 locations × 3 principal climate components). We used Ward's hierarchical clustering algorithm with a Euclidean distance of standardized principal components (i.e., a Mahalanobis distance metric), implemented with the hclust package for the R programming environment.

3 | RESULTS

3.1 | Ensemble selection

There were 44 models in the CMIP6 ScenarioMIP holdings as of December 15, 2020 (Table 1). Twelve of these candidates were excluded because they did not provide monthly means of T_{min} and T_{max} (Criterion 1). Notably, CESM2 does provide T_{min} and T_{max} in its future projections, but due to an archiving error these variables are not available for historical runs. An additional 11 models were excluded because they had less than three historical runs (Criterion 2) or an incomplete scenario set (Criterion 3). Of the 21 models that passed these first three objective criteria, we excluded two more models on the basis of having a clear choice between models from the same institution (Criterion 4): CanESM5-CanOE in favour of CanESM5 and EC-Earth3-Veg in favour of EC-Earth3. In addition, of the several variants of the GISS-E2-1-G model, we selected the r*i1p3f1 variant because it had the most complete set of scenario simulations. We downloaded historical simulations from the remaining 19 models for further evaluation. For practical purposes, we limited downloads to 5 historical simulations for EC-Earth3 due to its relatively high resolution, and 10 simulations for other models.

To assist with choosing among models from the same institution (Criterion 4) or with shared components (Criterion 5), we conducted an analysis of bias in T_{min}, T_{max}, and precipitation (Figure 1). We excluded AWI-CM-1-1-MR on the sole basis of its very high temperature
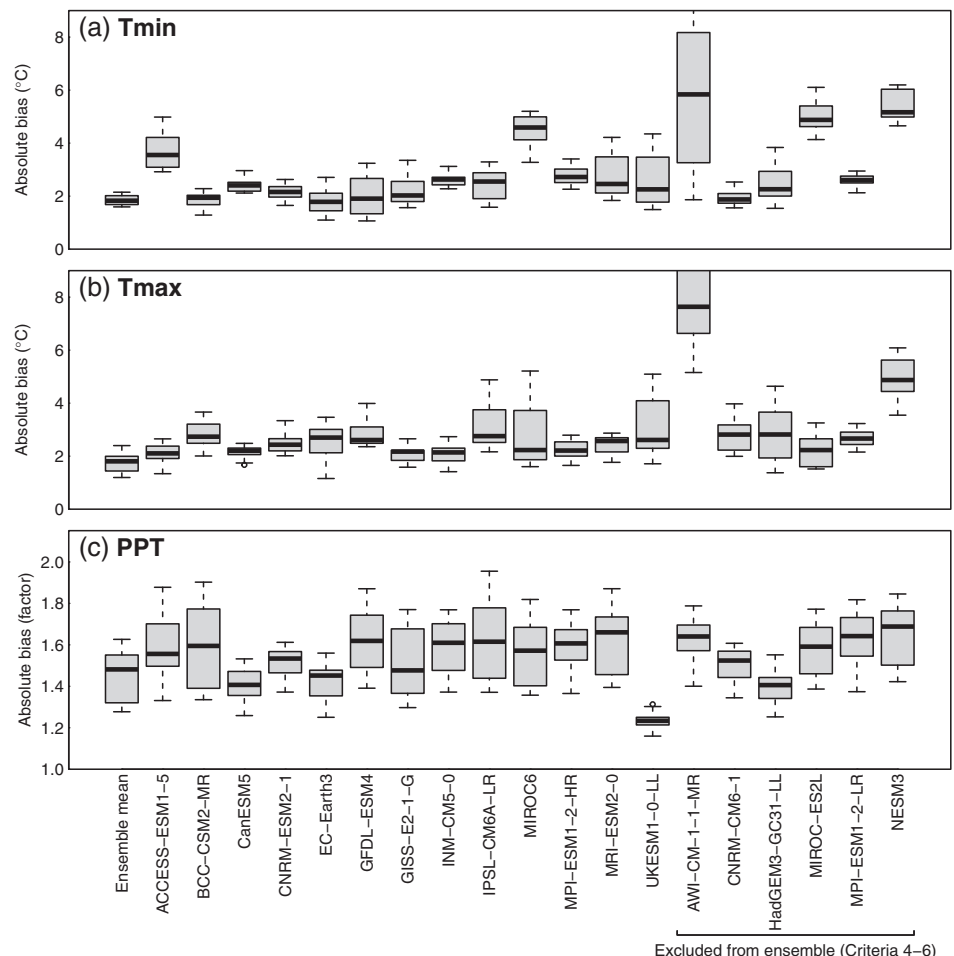

FIGURE 1 Model biases in monthly means of (a) daily minimum temperature, (b) daily maximum temperature, and (c) precipitation. Each box represents 12 values of mean absolute bias over North America, one for each month. Absolute bias for precipitation is expressed as a factor of magnitude. For example, relative biases of 50 and 200% both have an absolute bias of 2

TABLE 2 Institution and citation for each model in the 13-model ensemble

Model	Institutions	Citation
ACCESS-ESM1.5	Commonwealth Scientific and Industrial Research Organisation (Australia)	Ziehn *et al.* (2020)
BCC-CSM2	Beijing Climate Center (China)	Wu *et al.* (2019)
CanESM5	Canadian Centre for Climate Modelling and Analysis (Canada)	Swart *et al.* (2019)
CNRM-ESM2-1	CNRM (Centre National de Recherches Meteorologiques) and CERFACS (Centre Europeen de Recherche et de Formation Avancee en Calcul Scientifique) (France)	Séférian *et al.* (2019)
EC-Earth3	EC-Earth Consortium (European Community)	Döscher *et al.* (2021)
GFDL-ESM4	National Oceanic and Atmospheric Administration, Geophysical Fluid Dynamics Laboratory (USA)	Dunne *et al.* (2020)
GISS-E2.1	Goddard Institute for Space Studies (USA)	Kelley *et al.* (2020)
INM-CM5.0	Institute for Numerical Mathematics (Russia)	Volodin *et al.* (2017)
IPSL-CM6A-LR	Institut Pierre Simon Laplace (France)	Boucher *et al.* (2020)
MIROC6	JAMSTEC (Japan Agency for Marine-Earth Science and Technology), AORI (Atmosphere and Ocean Research Institute), NIES (National Institute for Environmental Studies), and R-CCS (RIKEN Center for Computational Science) (Japan)	Tatebe *et al.* (2018)
MPI-ESM1.2-HR	Max Planck Institute for Meteorology (Germany)	Müller *et al.* (2018)
MRI-ESM2.0	Meteorological Research Institute (Japan)	Yukimoto *et al.* (2019)
UKESM1	Met Office Hadley Centre and Natural Environment Research Council (UK)	Sellar *et al.* (2019)

bias (Criterion 6). NESM3 also has high bias relative to the other models and was excluded due to shared components with MPI-ESM1 (Criterion 5). None of the other related models were sufficiently biased to warrant exclusion.

Final choices from among related models were: UKESM1.0-LL selected over HadGEM3-GC31-LL due to higher resolution and more simulations; MIROC6 over MIROC-ES2L due to higher number of runs and regionally high biases in the Pacific Northwest; MPI-ESM1.2-HR over MPI-ESM1-2-LR to improve representation of high-resolution models in the ensemble; and CNRM-ESM2-1 arbitrarily selected over CNRM-CM6-1 in favour of the earth system model (ESM) configuration. In summary, the six criteria reduced the 44 candidate models to a 13-model ensemble (Table 2).

3.2 | Attributes of the 13-model ensemble

3.2.1 | Representation of the full CMIP6 ensemble

The 13-model ensemble has a mean ECS of 3.7°C and a range of 1.9–5.6°C, which matches ECS of the full CMIP6 ensemble (3.7°C; 1.8–5.6°C) (Meehl *et al.*, 2020). The 13-model ensemble is moderately representative of

regional transient temperature and precipitation changes (2061–2100, SSP2-4.5) found in the larger 33-model CMIP6 ensemble (Figure 2), with some key exceptions. Two models in the larger ensemble are distinct outliers: KACE-1-0-G exhibits cooling over the contiguous US (WNA, CNA, and ENA regions) and Mexico (NCA region); and AWI-CM-1-1-MR exhibits an outlying 80% reduction in precipitation over CNA and NCA. We removed these two outlier models from further analysis of representation. Notwithstanding the outliers, the 13-model ensemble is conspicuously unrepresentative of the larger CMIP6 ensemble in summer precipitation change over western North America (WNA). The models with highest precipitation increases in this region, in decreasing order, are NorESM2-LM, NorESM2-MM, CESM2, and CESM2-WACCM. These four models were ineligible for inclusion in the selected ensemble because they did not archive T_{min} and T_{max}. The model exhibiting extreme drying in the WNA region is MPI-ESM1-2-LR, which was eligible but excluded in favour of MPI-ESM1-2-HR on the basis of higher spatial resolution in the latter. The content of Figure 2 can be explored interactively in the supplemental web application (https://bcgov-env.shinyapps.io/cmip6-NA/).

Within each IPCC region, there is considerable spatial variation in the selected ensemble's representation of the larger CMIP6 ensemble (Figure 3a–d). Representation of model-mean change is lower for precipitation (Figure 3a,
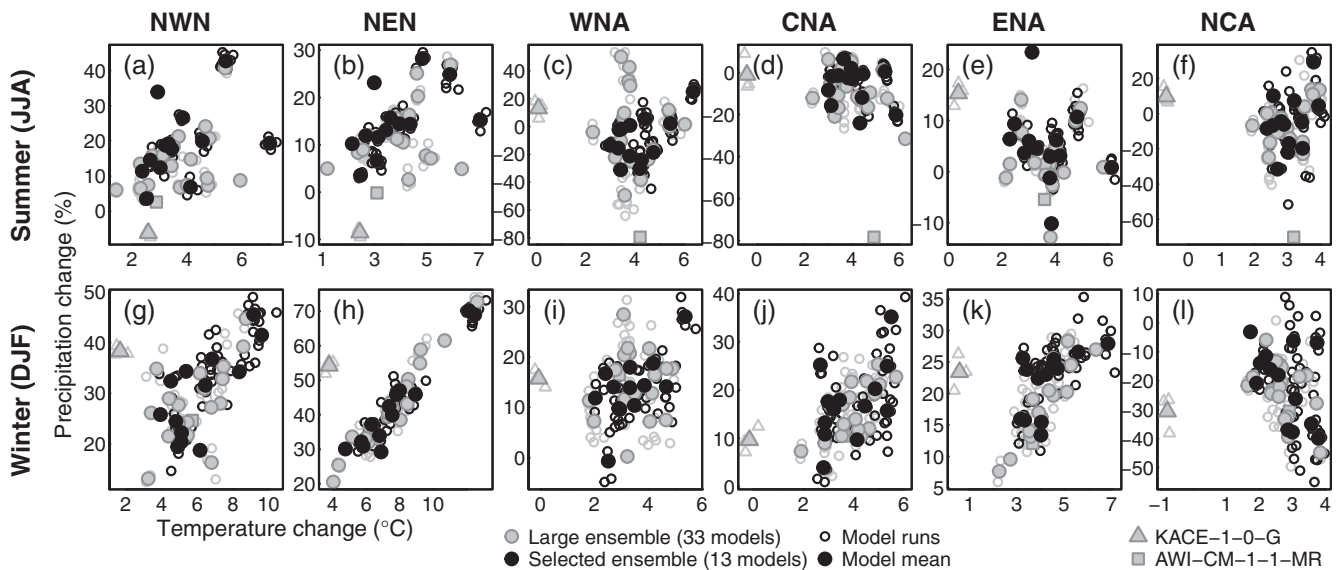
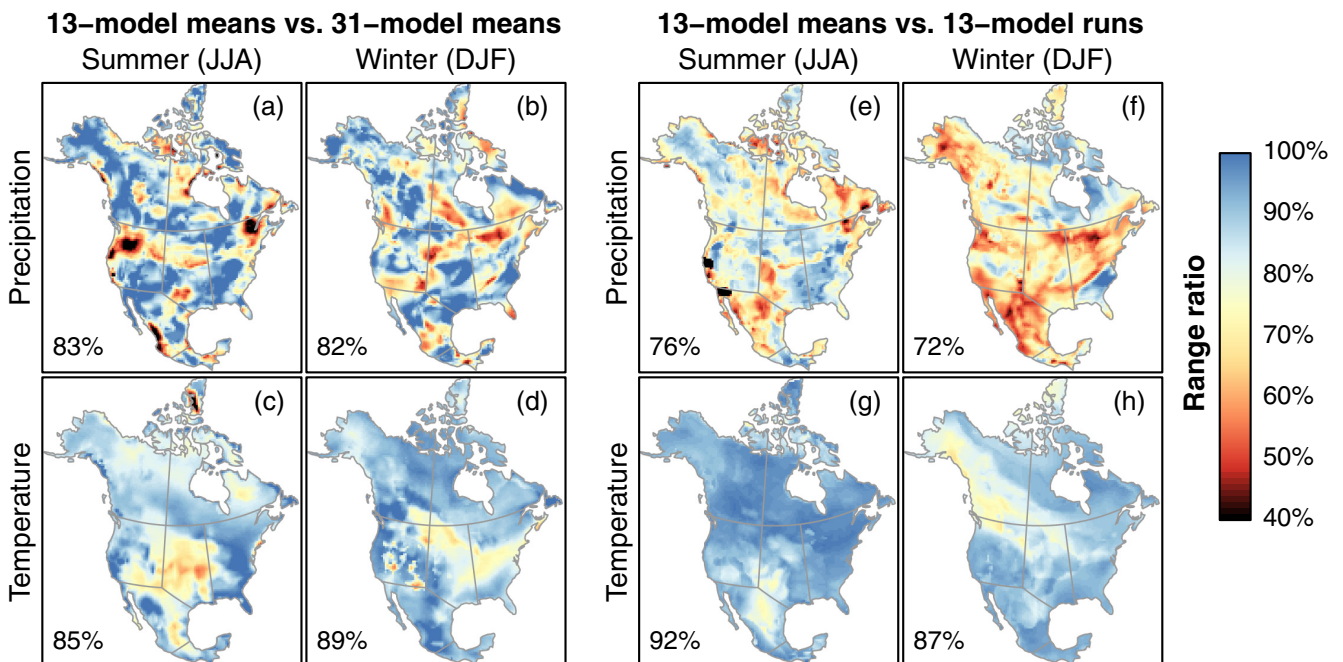**FIGURE 2** Representation of regional mean temperature and precipitation change in the selected 13-model ensemble relative to a larger 33-model CMIP6 ensemble. Individual model simulations (runs) are shown as open circles, and the single-model means of these simulations are shown as larger filled circles. Outlying models are given different symbols for ease of identification. Codes for IPCC regions of North America (Figure 7h) are northwestern (NWN), northeastern (NEN), western (WNA), central (CNA), eastern (ENA), and northern Central America (NCA)

FIGURE 3 Range of mean temperature and precipitation change in the selected 13-model ensemble relative to a larger 31-model CMIP6 ensemble. Change for each model simulation is the 2061–2100 mean SSP2-4.5 climate relative to the 1961–1990 mean of all historical simulations by the model. (a–d) Ratio of the range of single-model ensemble means in the 13-model and 31-model ensembles. (e–h) Ratio of the range of single-model ensemble means to the range of all individual simulations in the 13-model ensemble. Region boundaries are IPCC regions (Figure 7h) [Colour figure can be viewed at wileyonlinelibrary.com]

b) than for temperature (Figure 3c,d), and areas of poor representation of precipitation change are concentrated in subregions. Some of these areas may be due to natural variability in models with only one run. However, the prominent representation gap for summer precipitation change in the Pacific Northwest USA is induced by

exclusion of the NorESM, CESM2, and MPI-ESM1-2-LR models, all of which have multiple simulations and are therefore robust to natural variability. Reduced representation of the temperature change in central North America (Figure 3c,d) is associated with low warming in CAMS-CSM1-0 and high warming in HadGEM3-GC31-LL.

The range ratio analysis also provides a useful assessment of the degree to which the ensemble spread in individual model simulations (runs) is represented by the single-model means of these simulations (Figure 3e–h). Model means of temperature change are generally representative of the individual model runs, with exceptions of summer in northern Central America (Figure 3g) and winter in NW North America (Figure 3h). In contrast, model means of precipitation change are poorly representative of the variation in individual model runs, particularly in winter (Figure 3e,f).

3.2.2 | Projected climate change

A visual comparison of projected seasonal changes in T_{min}, T_{max}, and precipitation (Figure 4) indicates some basic attributes of the ensemble simulations. All models exhibit Arctic amplification of winter temperatures, though it is relatively subtle in EC-Earth3. Most models project the strongest summer warming at mid-latitudes. All models, with the exception of UKESM1, have a similar pattern of warming in T_{min} and T_{max}, though the magnitude of warming is greater for T_{min} in most models.

Continental-scale patterns of winter (December–February) precipitation change are somewhat consistent among models, with declines in Mexico and increases in the Arctic and Boreal regions. Deviations from this pattern are strongest in models with few (1–3) historical runs for SSP2-4.5 (BCC-CSM2-MR, GFDL-ESM4, and INM-CM5.0), likely due to internal variability. This result emphasizes the benefit of multiple runs in smoothing out natural variability to reveal the anthropogenic climate change signal in noisy climate variables like precipitation and winter temperature.

Most models project a reduction in summer precipitation in the coastal areas of the Pacific Northwest (California, Oregon, Washington, and southern BC). There is substantial disagreement among models in summer precipitation change over the rest of the continent. The muted summer precipitation change in the ensemble mean hides this ensemble disagreement, and underscores the importance of assessing climate change impacts with an ensemble of model projections rather than solely using the ensemble mean.

The two high-ECS models CanESM5 and UKESM1 have similar patterns and magnitudes of change in winter temperature and precipitation. However, they differ substantially in the summer, with UKESM1 showing much higher increases in daytime temperatures (T_{max}) in temperate and boreal regions and stronger declines in precipitation in central North America. Although CanESM5 has a higher ECS and stronger trend in 1970–2014 global heating (Liang et al., 2020), UKESM1 projects stronger mid-century heating over North America.

3.2.3 | Spatial resolution and model orography

The selected 13-model ensemble has a mean latitudinal grid resolution of 1.4° (range of 0.7°–2.8°) (Figure 5). Four models (EC-Earth3, GFDL-ESM4, MPI-ESM1.2-HR, and MRI-ESM2.0) resolve the macrotopography of the Western Cordillera, namely the Sierra Nevada, Cascade Range, Rocky Mountains, and British Columbia (BC) Coast Ranges. BCC-CSM2-MR does not resolve these ranges, despite having sufficient grid resolution to do so. CanESM5 has a distinctly low resolution of 2.8° × 2.8°.

3.2.4 | Elevation-dependent warming

There are large differences among models in the representation of elevation-dependent warming (EDW). These differences are illustrated using spring (MAM) T_{max} in a subset of the ensemble over the Coast Range and Rocky Mountains of southwestern Canada (Figure 6). EC-Earth3 and MRI-ESM2.0 both resolve these mountain ranges in their model orography (Figure 6a,d). EC-Earth3 has a strong signal of elevation-dependent warming over the Coast Range and Rocky Mountains, with more than double the warming in the Rocky Mountains than the adjacent plateaus (Figure 6b,c). MRI-ESM2.0 exhibits a relatively weak relationship between elevation and warming (Figure 6e, f). ACCESS-ESM1.5 and MIROC6 represent models with lower spatial resolution that represent the Coast Range and Rocky Mountains as a single feature in their model orography. ACCESS-ESM1.5 does not exhibit EDW. MIROC6 has a strong EDW signal despite being a moderate-resolution model with no differentiation of the two mountain ranges. The example of spring T_{max} is purely illustrative and does not represent each model's EDW in other elements and seasons. For example, the pattern of EDW among models is reversed for summer T_{min} (not shown), where MRI-ESM2.0 and ACCESS-ESM1.5 exhibit EDW, while EC-Earth3 and MIROC6 do not.
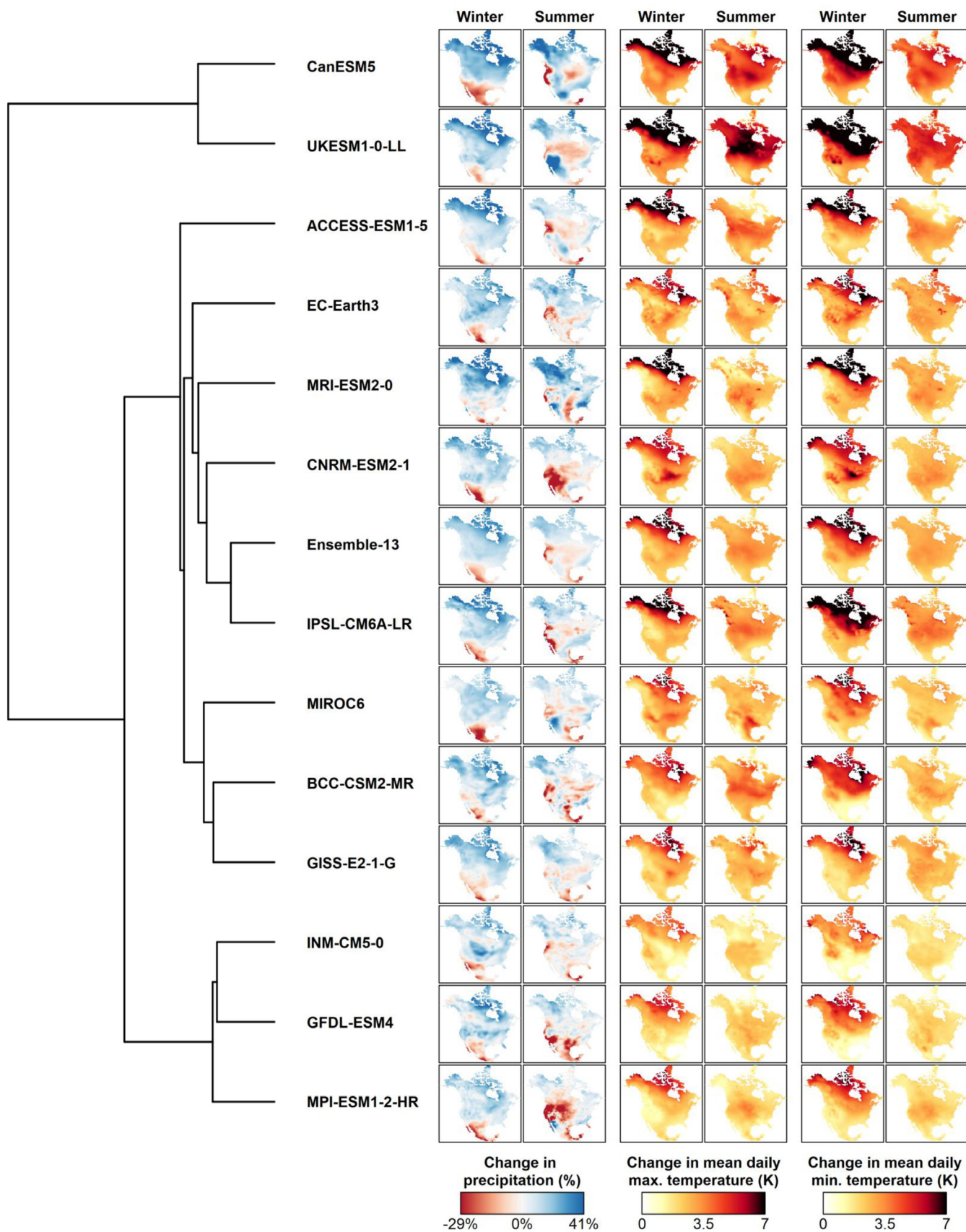
FIGURE 4 Spatial variation in climate change responses among the 13-model ensemble. Mapped climate changes are for the mean projected climate of the 2041–2060 period (SSP2-4.5). Precipitation is log-scaled to provide proportional magnitude of positive and negative changes. Models are structured by a cluster dendrogram of spatial similarity in seasonal climate changes in all three climate elements [Colour figure can be viewed at wileyonlinelibrary.com]
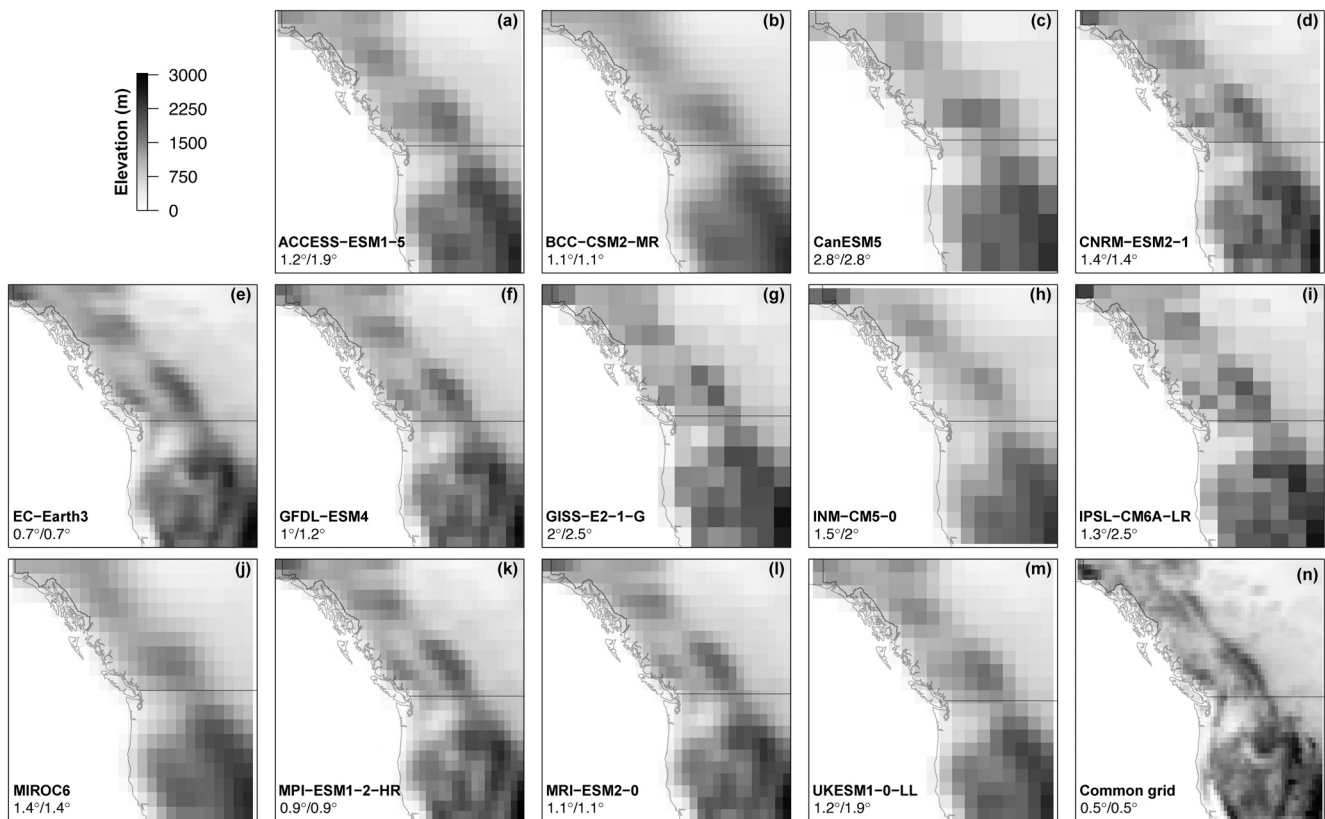
FIGURE 5 Effective topographic resolution of the 13 selected models. (a–m) Model orography (elevation of land surface) in the native grid of each model. The extent of the map is central-western North America (106 –142 W, 37 –62 N). The common grid (panel n) is the 0.5° grid used for extraction of observations from ClimateNA for the purpose of the bias assessment

3.2.5 | Diurnal temperature range

The models consistently underestimate the diurnal temperature range (DTR), measured as the difference between T_{min} and T_{max} (Figure 7). However, the 13-model ensemble and the 8-model subset (described in section 3.3.2) reproduce the observed seasonal cycle in all regions. Models that deviate most from the ensemble mean seasonal cycle generally are those excluded from the 8-model subset, namely IPSL-CM6A-LR (high amplitude in Arctic regions and underestimated elsewhere), BCC-CSM2-MR (high amplitude at mid-latitudes), and UKESM1-0-LL (high amplitude in Arctic regions and WNA). Among the 8-model subset, MIROC6 is distinct in overestimating the amplitude of the seasonal cycle in most regions.

3.3 | Ensemble subset selection

3.3.1 | Screening exclusions

The following four models are prioritized for exclusion from subsets of the ensemble based on combinations of

the four screening criteria: (a) *CanESM5*, due to its very high climate sensitivity (Criterion 6) and its very low horizontal resolution (Criterion 8); (b) *INM-CM5.0*, because it has very low climate sensitivity (ECS 1.9°C) and is an outlier among CMIP6 models for under-representing the observed 1975–2014 global temperature trend (Liang *et al.*, 2020) (Criterion 7). In addition, this model has only one simulation for most scenarios, producing a less robust climate signal (Criterion 9); (c) *BCC-CSM2-MR*, due to having a single simulation for each scenario (Criterion 9) and low topographic resolution (Criterion 8); and (d) *IPSL-CM6A-LR*, due to isolated grid cells with very high summer warming in the BC Coast Ranges and Southeast Alaska (Figure 8; Criterion 10). The warming in these cells may be physically plausible in the model's simplified topography, but is problematic for downscaling to higher spatial resolutions.

UKESM1 also has very high climate sensitivity (Criterion 7), similar to CanESM5, that is assessed by the IPCC as very unlikely based on observational evidence (Sherwood *et al.*, 2020; Arias *et al.*, 2021). Some researchers may wish to constrain their ensemble subset to observations by excluding this model. Others may wish
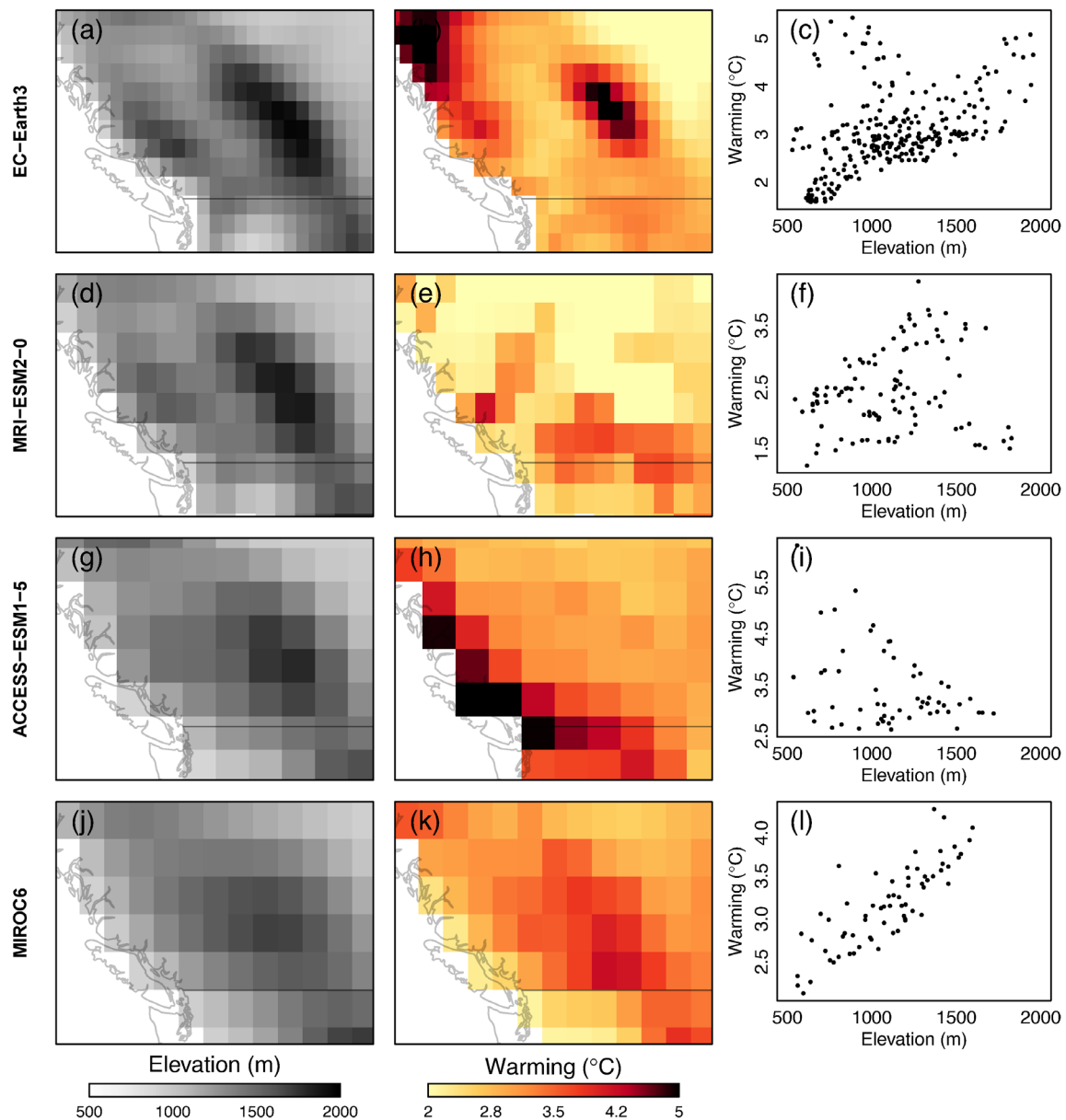
FIGURE 6   Relationships between elevation and warming (spring (MAM) T_{max}) over southwestern Canada in four CMIP6 models. Projected warming is for the 2061–2080 period under SSP2-4.5 for all models. Coastal cells (elevation <500 m) are excluded to reduce the maritime influence on the analysis [Colour figure can be viewed at wileyonlinelibrary.com]

to include a high-sensitivity model in their subset as a representation of the long tail of uncertainty in the upper limit of climate sensitivity (Sutton, 2018). To accommodate both perspectives, we provide ordered subsets with and without UKESM1 in the ordered ensemble subsets. We preferred UKESM1 over CanESM5 as a representative of high-sensitivity models due to its higher grid resolution and closer alignment with the observed post-1970 global heating trend (Liang *et al.*, 2020).

The resulting 8-model subset is ACCESS-ESM1.5, CNRM-ESM2-1, EC-Earth3, GFDL-ESM4, GISS-E2-1-G, MIROC6, MPI-ESM1.2-HR, and MRI-ESM2.0. This 8-model ensemble has a mean global ECS of 3.4°C

(2.6–4.8°C), using ECS values provided by Meehl *et al.* (2020). The 9-model subset that includes UKESM1 has a mean global ECS of 3.6°C (2.6–5.4°C).

3.3.2 | Ordered subsets

Table 3 specifies ordered subsets of the models that passed screening criteria 7–10. For a desired region and subset size, the ensemble subset for each region includes all models listed at and above the desired subset size. For example, a 4-model ensemble for the NEN region would include CNRM-ESM2-1, UKESM1.0-LL, EC-Earth3, and
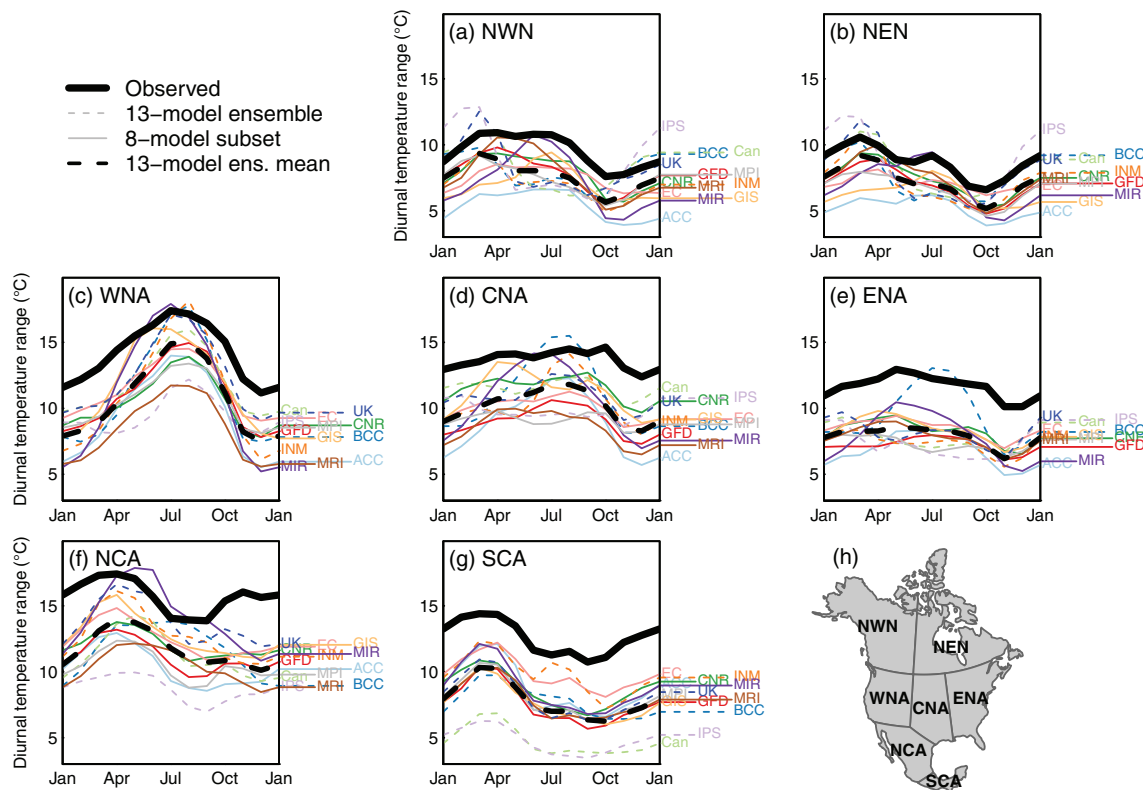
FIGURE 7 Seasonal cycle of the mean diurnal temperature range in observations and the 13-model ensemble, averaged over each IPCC reference region (h) (Iturbide *et al.*, 2020). Mean diurnal temperature range is calculated as the difference between monthly 1961–1990 normals of T_{min} and T_{max}. Observations are the ClimateNA composite of PRISM and WorldClim gridded climate normals (Wang *et al.*, 2016). Model abbreviations are the first two to three letters of the model name [Colour figure can be viewed at wileyonlinelibrary.com]

MPI-ESM1.2-HR. The considerable variation among regions in the order of the subsets underscores the spatial variation in climate change responses across North America. The exception to this variation in model order is that UKESM1 is the second model in all regions in the 9-model subset. Since the first position in the order is the model closest to the ensemble centroid and the second position is the model furthest from the centroid, this result indicates that UKESM1 projects the most extreme climate changes in all IPCC reference regions of North America.

4 | DISCUSSION

We selected 13 CMIP6 models from a candidate pool of 44 models contributing to the CMIP6 experiment. This 13-model ensemble is representative of the distribution of equilibrium climate sensitivity in the full CMIP6 ensemble and adequately represents the CMIP6 range of transient regional changes in precipitation and temperature. The 13-model ensemble facilitates robust downscaling by using multiple historical simulations per scenario for each model and excluding models with high bias. We

provided rationale for an 8-member subset of the ensemble based on screening criteria and order these 8 models for selection of smaller ensembles for regional analysis in North America. We also highlighted some tradeoffs among the models in terms of grid resolution, number of simulation runs, climate sensitivity, regional biases, and local artefacts. These results, and the accompanying web application (https://bcgov-env.shinyapps.io/cmip6-NA/), help readers to make model selections appropriate to their specific research objectives.

4.1 | Model bias

The bias assessment was a useful way to identify models with extreme divergence from the observed climate. Exceptionally high temperature biases were a sufficient reason for the exclusion of AWI-CM1-1-1-MR. High temperature biases are an attribute of concern in two of the models selected for the ensemble, ACCESS-ESM1.5 and MIROC6, but without a process evaluation are not sufficient basis for exclusion. The moderate biases in the rest of the ensemble, however, do not necessarily indicate a problem with the models. Bias is the difference between model simulations
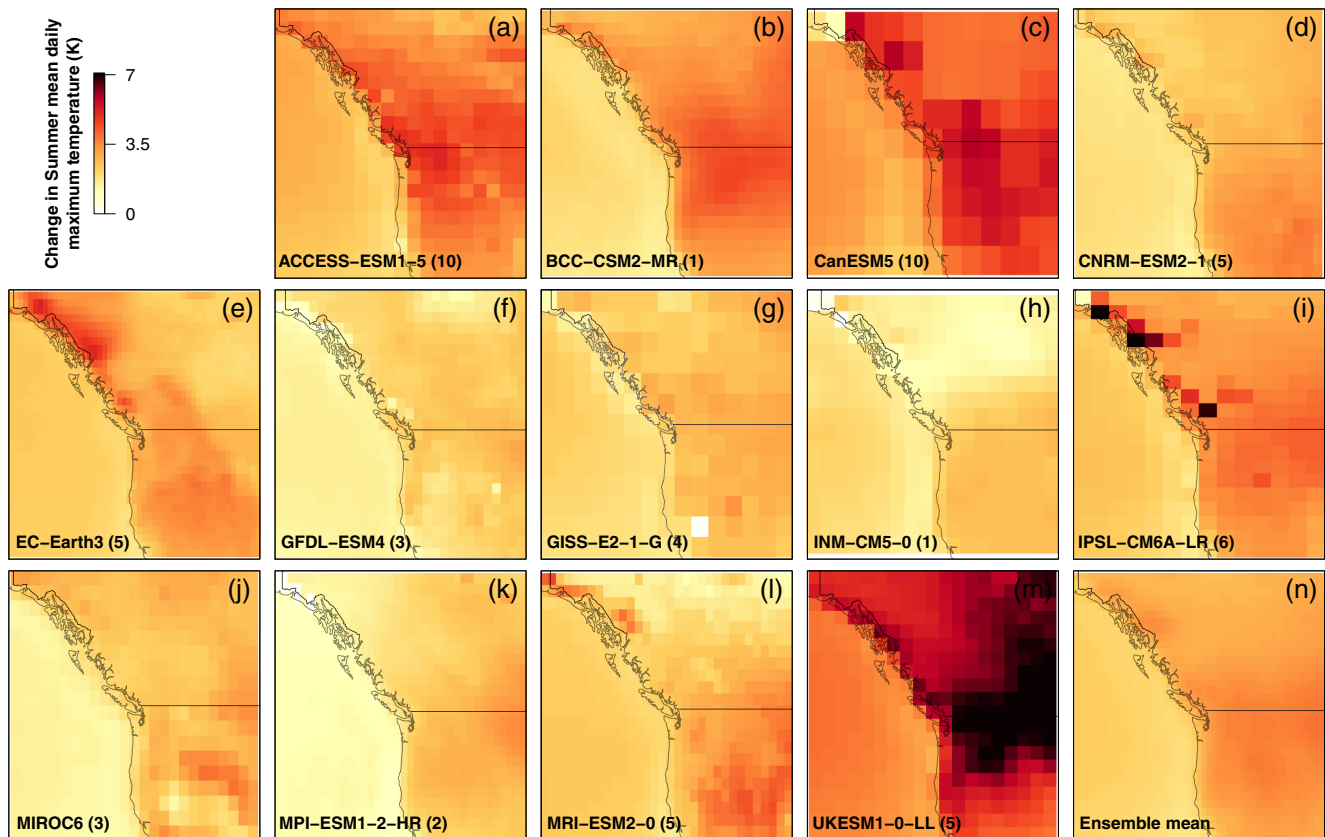
FIGURE 8 Summer (JJA) daytime warming in the 13-model ensemble over central-western North America (106 –142 W, 37 –62 N). Values are the change in summer T_{max} for the 2041–2060 period (SSP2-4.5), relative to 1961–1990, in the native model grid. Change is calculated from the mean of multiple simulation runs per model, specified next to the model name [Colour figure can be viewed at wileyonlinelibrary.com]

and the observed climate. We controlled the confounding influence of natural variability in each model by calculating bias using the mean of several simulation runs. This measure is not possible for observations since there is only one realization of the observed climate. Natural variability in the observed climate, therefore, could produce the appearance of bias even in a hypothetical "perfect" model (Lanzante *et al*., 2018). The ensemble mean absolute bias of 2°C in temperature and by a factor of 1.5 in precipitation cannot be definitively attributed to the models or the ensemble; it is to some extent an artefact of natural variability in the observed climate. A process-based evaluation of models (e.g., Karmalkar *et al*., 2019) can be helpful in further assessing the reliability of individual models for specific purposes and regions.

4.2 | Representation of climate change uncertainty

Climate change uncertainty can be decomposed into three components: scenario uncertainty, modelling (process) uncertainty, and internal (natural) variability (Hawkins

and Sutton, 2009). Ideally, a small multimodel ensemble like the one selected here should conserve these uncertainties as expressed in the larger ensemble of candidate simulations. We explicitly conserved scenario uncertainty by selecting models that provide simulations for the four core SSP marker scenarios. The 13-model ensemble adequately conserves modelling uncertainty—approximated globally by ECS and regionally by the range of model mean seasonal temperature and precipitation changes in a screened 31-model CMIP6 ensemble (Figures 2 and 3a–d)—with some regional exceptions. These exceptions should be noted as caveats for interpretation of regional climate change uncertainties in downstream analyses. Finally, we explicitly prioritized models that allow assessment and control of internal variability by selecting models with a minimum of three historical simulations. However, five of the selected models have only one or two simulations for each emissions scenario. For the purpose of representing modelling uncertainty, model means from these models should be assumed to be somewhat confounded by internal variability.

The internal variability component of uncertainty is only conserved if the individual simulations of each model

TABLE 3 Ordered subsets of the 13-model ensemble

Subset size	IPCC reference region							
	NEN	NWN	WNA	CNA	ENA	NCA	SCA	NAM
Including UKESM1-0-LL								
1	CNRM	CNRM	MRI	ACC	EC	MRI	GISS	CNRM
2	UK	UK	UK	UK	UK	UK	UK	UK
3	EC	EC	MPI	CNRM	GFDL	GFDL	ACC	GFDL
4	MPI	MPI	GISS	GFDL	MRI	EC	MIR	EC
5	MRI	ACC	EC	MIR	MIR	MIR	EC	MRI
6	ACC	GISS	CNRM	EC	GISS	CNRM	GFDL	GISS
7	GISS	MRI	MIR	GISS	MPI	MPI	MPI	MIR
8	GFDL	MIR	GFDL	MPI	ACC	ACC	CNRM	ACC
9	MIR	GFDL	ACC	MRI	CNRM	GISS	MRI	MPI
Excluding UKESM1-0-LL								
1	CNRM	CNRM	MRI	MRI	GISS	MRI	GISS	CNRM
2	EC	EC	MPI	GFDL	ACC	GFDL	ACC	GFDL
3	GFDL	ACC	GISS	MIR	MRI	EC	MIR	EC
4	MRI	MPI	MIR	CNRM	GFDL	MIR	EC	GISS
5	ACC	GISS	EC	GISS	CNRM	CNRM	GFDL	MIR
6	GISS	MIR	CNRM	EC	EC	MPI	MPI	ACC
7	MPI	MRI	GFDL	MPI	MIR	ACC	MRI	MRI
8	MIR	GFDL	ACC	ACC	MPI	GISS	CNRM	MPI

Note: Subsets are provided for North America (NAM) and the seven IPCC reference regions (Figure 7h). The order of each subset indicates the models recommended for each user-determined ensemble size. For example, a four-member ensemble for the NEN region would comprise CNRM, UK, EC, and MPI. Exclusion of UKESM1 provides an ensemble that is consistent with the IPCC AR6 assessed constraints on equilibrium climate sensitivity (Arias *et al.*, 2021). Model abbreviations are ACC (ACCESS-ESM1.5), CNRM (CNRM-ESM2-1), EC (EC-Earth3), GFDL (GFDL-ESM4), GISS (GISS-E2-1-G), MIR (MIROC6), MPI (MPI-ESM1.2-HR), MRI (MRI-ESM2.0), and UK (UKESM1.0-LL).

are provided in a downscaled ensemble. Downscaled climate normal products (e.g., ClimateNA and WorldClim2) typically provide model means calculated from multiple simulations, but not the individual simulations themselves. We demonstrated that the ensemble of model means obscures substantial internal variability in precipitation throughout the continent, and in temperature in specific regions and seasons (Figure 3e–h). In other words, an ensemble of model means artificially reduces climate change uncertainty (Deser *et al.*, 2012) and precludes assessment of the full range of potential climate impacts. Within the limits of practicality, it is preferable to provide multiple simulations of each model/scenario combination in products of downscaled climate normals.

4.3 | Grid resolution and elevation-dependent warming

Four of the models in the ensemble have horizontal grid resolution sufficient to resolve the major mountain ranges

of western North America. One model (EC-Earth3) has relatively high resolution ($0.7° \times 0.7°$) approaching the previous generation of regional climate models used for dynamical downscaling. The trend towards higher resolution is encouraging, but the benefits of moderate resolution models for km-scale downscaling are ambiguous. On one hand, resolving mountain ranges allows for stronger differentiation of maritime/continental transitions (Lanzante *et al.*, 2018), windward and leeward dynamics (Kanehama *et al.*, 2019), and elevation-dependent climate changes (Palazzi *et al.*, 2019). On the other hand, these resolved mountain ranges are still highly simplified features in even the highest resolution models in the ensemble. The higher-resolution models do not necessarily reduce the challenges of km-scale downscaling, but instead can shift these challenges to finer spatial scales.

Our case study of elevation-dependent warming (EDW) is an illustration of the trade-offs of increased grid resolution. EDW is a poorly-understood phenomenon with several hypothesized causes including the snow-albedo feedback, longwave water vapour feedbacks,

aerosols, and changes in cloud cover (Pepin *et al.*, 2015; Minder *et al.*, 2018; Palazzi *et al.*, 2019). The large differences in EDW evident among models in Figure 6 are unsurprising given the complexity of the phenomenon. In addition to the process uncertainties, however, grid resolution itself is a source of model variation in EDW. Since the drivers of EDW are local in scale, the simulation of EDW over the highly generalized topographies of global climate models is a source of error for downscaling: EDW will be applied uniformly to all locations—valley floors to mountain peaks—within a GCM grid cell during change-factor downscaling. The comparison of MIROC6 and EC-Earth3 demonstrates that increasing model resolution can reduce this source of error at regional scales (i.e., by resolving gaps between mountain ranges) while increasing it at local scales (i.e., by applying more fully resolved EDW to unresolved valleys). In the absence of additional downscaling measures to explicitly account for EDW and other localized climate change drivers, we do not view the higher-resolution models in the ensemble as intrinsically more valuable or valid. The tradeoffs of model resolution are a component of modelling uncertainty, and it is beneficial to include a range of grid resolutions in a downscaling ensemble.

4.4 | Diurnal temperature range

Underestimation of DTR is a persistent feature of climate models (Wang and Clow, 2020). Intermodel differences in DTR can be attributed to differences in parameterizations for clouds, aerosols and soil moisture, among others (Lindvall and Svensson, 2015). However, the consistent underestimation of DTR relative to observations has not been definitively explained. Part of the underestimation of DTR may be due to differences in the timescale of DTR measurement in observations and models; since $T_{\min}$ and $T_{\max}$ are measured instantaneously in observations but simulated over longer timesteps in models, models are expected to have lower DTR (Wilson *et al.*, 2008; Rupp *et al.*, 2013). To the extent that underestimation of DTR is an artefact of the different timescales of measurement in observations and models, rather than of systematic biases in the driving processes, some overestimation of $T_{\min}$ and underestimation of $T_{\max}$ would be expected even from a perfect model.

4.5 | Reconciling the equilibrium climate sensitivity of the ensemble with observational constraints

The 13-model ensemble selected here, like the full CMIP6 ensemble, has a mean (3.7°C) and upper limit (5.6°C) of

equilibrium climate sensitivity that substantially exceeds the IPCC AR6 assessed best estimate ECS of 3°C and *very likely* upper limit of 5°C (Arias *et al.*, 2021). In other words, the 13-model ensemble contains models that simulate stronger global warming than is supported by multiple lines of observational evidence. Five (38%) of the 13 models are above the IPCC AR6 assessed *likely* upper limit on ECS of 4°C, and two (15%) of the models are above the *very likely* upper limit of 5°C. If the ensemble were to strictly conform to the IPCC assessed range, there would be only two models exceeding 4°C ECS and no models exceeding 5°C, following the IPCC's probabilistic definitions of *likely* (one-sided $p > 83\%$) and *very likely* (one-sided $p > 95\%$).

The need to reconcile the CMIP ensemble ECS range with observational constraints is a new dilemma for climate change impacts and adaptation researchers. It is long been agreed that model democracy (one model, one vote) is not a strictly valid method of assessing climate change uncertainty (Knutti, 2010; Leduc *et al.*, 2016). However, prior to CMIP6 this objection was somewhat academic since the distribution of ECS in CMIP ensembles approximately matched the (wider) range of ECS supported by other lines of evidence (Schmidt, 2021). For practical purposes it was reasonable for analysts to use the multimodel ensemble spread in previous CMIP generations as a proxy for scientific uncertainty on climate change. This approach is no longer valid given the incongruence between the CMIP6 ensemble range of ECS and the IPCC assessed range (Schmidt, 2021). Careful model selection is now required to avoid biasing regional climate change analyses.

There are several viable approaches to constrain CMIP6 ensembles in downscaled regional analyses. Weighting the models based on observational constraints is possible for regional analyses (Ribes *et al.*, 2021). However, in practice many analyses will require simply selecting a subset of the CMIP6 ensemble that is closer to the IPCC assessed range, as we have done with the 8-model subset. The disadvantage of this approach is that it discards valuable information from the excluded models. The CanESM5 and UKESM1 models are advanced models from respected modelling centres, with demonstrated skill in modelling many Earth system processes (Eyring *et al.*, 2021). Expressing variables of interest relative to the amount of regional or global warming is a widely practiced technique that facilitates inclusion of high-ECS models by removing the timing of the warming as a factor in the ensemble spread (Arias *et al.*, 2021). It is conceivable that both techniques could be used in a single study; to use the 8-model ensemble for time-relevant analyses and a larger ensemble for analyses where the warming level is more relevant. These

considerations highlight that the full CMIP6 ensemble is a somewhat arbitrary collection of non-independent models, and careful ensemble selection is necessary to achieve a meaningful representation of modelling uncertainty.

5 | CONCLUSION

Use of downscaled global climate model projections is expanding rapidly as climate change vulnerability assessments and adaptation planning become mainstream in many sectors. This increasingly diverse user base can benefit from a basic understanding of the attributes and limitations of the climate model output they are working with. The results of this study reinforce several best practices for the selection and use of global climate models for high spatial resolution downscaling of climate normals:

- The ensemble must be observationally constrained to be meaningful. The CMIP6 ensemble and the 13-model ensemble have a biased distribution of equilibrium climate sensitivities. This bias can be addressed by model exclusions (as in our 8-model subset), model weighting, or analysis relative to global warming levels rather than time.
- An ensemble of multiple models is essential for impact analysis; the ensemble mean projection alone can be misleading. For example, small summer precipitation changes indicated by the ensemble mean throughout North America are an artefact of averaging across much larger opposing trends among the models.
- Downscaled climate data products should include multiple simulations of each model/scenario combination. This allows downstream analyses to account for the contribution of natural variability to climate change uncertainty.
- Higher grid resolution is not necessarily better. Increased grid resolution can intensify downscaling errors in some locations while reducing them in others. A range of grid resolutions is desirable in a multimodel ensemble.
- Small ensembles should be used with caution. Even the 13-model ensemble leaves region-specific gaps in the distribution of climate changes projected by the full CMIP6 ensemble. Users of downscaled data can benefit from tools to identify these gaps for their variables and regions of interest.

CONFLICT OF INTEREST
The authors declare no potential conflict of interest.

AUTHOR CONTRIBUTIONS
Colin R. Mahony: Conceptualization; formal analysis; methodology; software; visualization; writing – original draft. **Tongli Wang:** Conceptualization; data curation. **Andreas Hamann:** Conceptualization; formal analysis; writing – review and editing. **Alex J. Cannon:** Methodology; software; writing – review and editing.

DATA AVAILABILITY STATEMENT
A supplementary web application (https://bcgov-env.shinyapps.io/cmip6-NA/) provides tools for model selection and visualization of the ensemble. Downscaled projections for the selected 13 CMIP6 models are available in ClimateNA (http://climatena.ca/), which provides downscaling at user-specified spatial resolution and various temporal intervals (annual, 20-year and 30-year periods). In addition to the basic monthly values of Tmin, Tmax, and precipitation, ClimateNA uses these elements to estimate derived bioclimatic and engineering variables such as heat sums and frost periods. Gridded (1-km) climate normals for the 8-model subset are provided at https://adaptwest.databasin.org/pages/adaptwest-climatena/.

ORCID
Colin R. Mahony https://orcid.org/0000-0002-6111-5675
Tongli Wang https://orcid.org/0000-0002-9967-6769
Andreas Hamann https://orcid.org/0000-0003-2046-4550
Alex J. Cannon https://orcid.org/0000-0002-8025-3790

REFERENCES
Arias, P.A., Bellouin, N., Coppola, E., Jones, R.G., Krinner, G., Marotzke, J., Naik, V., Palmer, M.D., Plattner, J.G.-K., Rogelj, M.R., Sillmann, J., Storelvmo, T., Thorne, P.W., Trewin, B., Rao, K.A., Adhikary, B., Allan, R.P., Armour, K., Bala, G., Barimalala, R., Berger, S., Canadell, J.G., Cassou, C., Cherchi, A., Collins, W., Collins, W.D., Connors, S.L., Corti, S., Cruz, F., Dentener, F.J., Dereczynski, C., Di Luca, A., Niang, A. D., Doblas-Reyes, F.J., Dosio, A., Douville, H., Engelbrecht, F., Eyring, V., Fischer, E., Forster, P., Fox-Kemper, B., Fuglestvedt, J.S., Fyfe, J.C., Gillett, N.P., Goldfarb, L., Gorodetskaya, I., Gutierrez, J.M., Hamdi, R., Hawkins, E.,

Hewitt, H.T., Hope, P., Islam, A.S., Jones, C., Kaufman, D.S., Kopp, R.E., Kosaka, Y., Kossin, J., Krakovska, S., Lee, J.-Y., Li, J., Mauritsen, T., Maycock, T.K., Meinshausen, M., Min, S.-K., Monteiro, P.M.S., Ngo-Duc, T., Otto, F., Pinto, I., Pirani, A., Raghavan, K., Ranasinghe, R., Ruane, A.C., Ruiz, L., Sallée, J.-B., Samset, B.H., Sathyendranath, S., Seneviratne, S.I., Sörensson, A.A., Szopa, S., Takayabu, I., Treguier, A.-M., van den Hurk, B., Vautard, R., von Schuckmann, S.Z.K., Zhang, X. and Zickfeld, K. (2021) Technical summary. In: Masson-Delmotte, P.Z., Pirani, A., Connors, S.L., Péan, C., Berger, S., Caud, N., Chen, Y., Goldfarb, L., Gomis, M.I., Huang, M., Leitzell, K., Lonnoy, E., Matthews, J.B.R., Maycock, T.K., Waterfield, T., Yelekçi, O., Yu, R. and Zhou, B. (Eds.) *Climate Change 2021: The Physical Science Basis. Contribution of Working Group I to the Sixth Assessment Report of the Intergovernmental Panel on Climate Change.* Cambridge and New York, NY: Cambridge University Press, pp. 1–150.

Boucher, O., Servonnat, J., Albright, A.L., Aumont, O., Balkanski, Y., Bastrikov, V., Bekki, S., Bonnet, R., Bony, S., Bopp, L., Braconnot, P., Brockmann, P., Cadule, P., Caubel, A., Cheruy, F., Codron, F., Cozic, A., Cugnet, D., D'Andrea, F., Davini, P., de Lavergne, C., Denvil, S., Deshayes, J., Devilliers, M., Ducharne, A., Dufresne, J.L., Dupont, E., Éthé, C., Fairhead, L., Falletti, L., Flavoni, S., Foujols, M.A., Gardoll, S., Gastineau, G., Ghattas, J., Grandpeix, J.Y., Guenet, B., Guez, L.E., Guilyardi, E., Guimberteau, M., Hauglustaine, D., Hourdin, F., Idelkadi, A., Joussaume, S., Kageyama, M., Khodri, M., Krinner, G., Lebas, N., Levavasseur, G., Lévy, C., Li, L., Lott, F., Lurton, T., Luyssaert, S., Madec, G., Madeleine, J.B., Maignan, F., Marchand, M., Marti, O., Mellul, L., Meurdesoif, Y., Mignot, J., Musat, I., Ottlé, C., Peylin, P., Planton, Y., Polcher, J., Rio, C., Rochetin, N., Rousset, C., Sepulchre, P., Sima, A., Swingedouw, D., Thiéblemont, R., Traore, A.K., Vancoppenolle, M., Vial, J., Vialard, J., Viovy, N. and Vuichard, N. (2020) Presentation and evaluation of the IPSL-CM6A-LR climate model. *Journal of Advances in Modeling Earth Systems*, 12, 1–52.

Brunner, L., Pendergrass, A.G., Lehner, F., Merrifield, A.L., Lorenz, R. and Knutti, R. (2020) Reduced global warming from CMIP6 projections when weighting models by performance and independence. *Earth System Dynamics*, 11, 995–1012.

Cannon, A.J. (2015) Selecting GCM scenarios that span the range of changes in a multimodel ensemble: application to CMIP5 climate extremes indices. *Journal of Climate*, 28, 1260–1267.

Cannon, A.J. (2018) Multivariate quantile mapping bias correction: an N-dimensional probability density function transform for climate model simulations of multiple variables. *Climate Dynamics*, 50, 31–49.

Deser, C., Knutti, R., Solomon, S. and Phillips, A.S. (2012) Communication of the role of natural variability in future North American climate. *Nature Climate Change*, 2, 775–779.

Döscher, R., Acosta, M., Alessandri, A., Anthoni, P., Arneth, A., Arsouze, T., Bergmann, T., Bernadello, R., Bousetta, S., Caron, L.-P., Carver, G., Castrillo, M., Catalano, F., Cvijanovic, I., Davini, P., Dekker, E., Doblas-Reyes, F., Docquier, D., Echevarria, P., Fladrich, U., Fuentes-Franco, R., Gröger, M., Hardenberg, J.V., Hieronymus, J., Karami, M.P., Keskinen, J.-P., Koenigk, T., Makkonen, R., Massonnet, F., Ménégoz, M., Miller, P., Moreno-Chamarro, E., Nieradzik, L., van Noije, T., Nolan, P., O'Donnell, D., Ollinaho, P., van den

Oord, G., Ortega, P., Prims, O.T., Ramos, A., Reerink, T., Rousset, C., Ruprich-Robert, Y., Le Sager, P., Schmith, T., Schrödner, R., Serva, F., Sicardi, V., Madsen, M.S., Smith, B., Tian, T., Tourigny, E., Uotila, P., Vancoppenolle, M., Wang, S., Wårlind, D., Willén, U., Wyser, K., Yang, S., Yepes-Arbós, X. and Zhang, Q. (2021) The EC-Earth3 earth system model for the Climate Model Intercomparison Project 6. *Geoscientific Model Development Discussions*, 1–90. https://doi.org/10.5194/gmd-2020-446

Dunne, J.P., Horowitz, L.W., Adcroft, A.J., Ginoux, P., Held, I.M., John, J.G., Krasting, J.P., Malyshev, S., Naik, V., Paulot, F., Shevliakova, E., Stock, C.A., Zadeh, N., Balaji, V., Blanton, C., Dunne, K.A., Dupuis, C., Durachta, J., Dussin, R., Gauthier, P.P. G., Griffies, S.M., Guo, H., Hallberg, R.W., Harrison, M., He, J., Hurlin, W., McHugh, C., Menzel, R., Milly, P.C.D., Nikonov, S., Paynter, D.J., Ploshay, J., Radhakrishnan, A., Rand, K., Reichl, B. G., Robinson, T., Schwarzkopf, D.M., Sentman, L.T., Underwood, S., Vahlenkamp, H., Winton, M., Wittenberg, A.T., Wyman, B., Zeng, Y. and Zhao, M. (2020) The GFDL Earth System Model version 4.1 (GFDL-ESM 4.1): overall coupled model description and simulation characteristics. *Journal of Advances in Modeling Earth Systems*, 12, e2019MS002015.

Eyring, V., Bony, S., Meehl, G.A., Senior, C.A., Stevens, B., Stouffer, R. J. and Taylor, K.E. (2016) Overview of the Coupled Model Intercomparison Project Phase 6 (CMIP6) experimental design and organization. *Geoscientific Model Development*, 9, 1937–1958.

Eyring, V., Gillett, N.P., Rao, K.M.A., Barimalala, R., Parrillo, M.B., Bellouin, N., Cassou, C., Durack, P.J., Kosaka, Y., McGregor, S., Min, S., Morgenstern, O. and Sun, Y. (2021) Human influence on the climate system. In: Masson-Delmotte, V., Zhai, P., Pirani, A., Connors, S.L., Péan, C., Berger, S., Caud, N., Chen, Y., Goldfarb, L., Gomis, M.I., Huang, M., Leitzell, K., Lonnoy, E., Matthews, J.B.R., Maycock, T.K., Waterfield, T., Yelekçi, O., Yu, R. and Zhou, B. (Eds.) *Climate Change 2021: The Physical Science Basis. Contribution of Working Group I to the Sixth Assessment Report of the Intergovernmental Panel on Climate Change.* Cambridge and New York, NY: Cambridge University Press, pp. 1–202.

Fick, S.E. and Hijmans, R.J. (2017) WorldClim 2: new 1-km spatial resolution climate surfaces for global land areas. *International Journal of Climatology*, 37, 4302–4315.

Hamann, A., Wang, T., Spittlehouse, D.L. and Murdock, T.Q. (2013) A comprehensive, high-resolution database of historical and projected climate surfaces for western North America. *Bulletin of the American Meteorological Society*, 94, 1307–1309.

Hawkins, E. and Sutton, R. (2009) The potential to narrow uncertainty in regional climate predictions. *Bulletin of the American Meteorological Society*, 90, 1095–1107.

Hijmans, R.J., Cameron, S.E., Parra, J.L., Jones, P.G. and Jarvis, A. (2005) Very high resolution interpolated climate surfaces for global land areas. *International Journal of Climatology*, 25, 1965–1978.

Hunter, R.D. and Meentemeyer, R.K. (2005) Climatologically aided mapping of daily precipitation and temperature. *Journal of Applied Meteorology*, 44, 1501–1510.

Iturbide, M., Gutiérrez, J.M., Alves, L.M., Bedia, J., Cerezo-Mota, R., Cimadevilla, E., Cofiño, A.S., Di Luca, A., Faria, S.H., Gorodetskaya, I.V., Hauser, M., Herrera, S., Hennessy, K., Hewitt, H.T., Jones, R.G., Krakovska, S., Manzanas, R., Martínez-Castro, D., Narisma, G.T., Nurhati, I.S., Pinto, I.,

Seneviratne, S.I., van den Hurk, B. and Vera, C.S. (2020) An update of IPCC climate reference regions for subcontinental analysis of climate model data: definition and aggregated datasets. *Earth System Science Data*, 12, 2959–2970.

Kanehama, T., Sandu, I., Beljaars, A., van Niekerk, A. and Lott, F. (2019) Which orographic scales matter most for medium-range forecast skill in the Northern Hemisphere winter? *Journal of Advances in Modeling Earth Systems*, 11, 3893–3910.

Karmalkar, A.V. (2018) Interpreting results from the NARCCAP and NA-CORDEX ensembles in the context of uncertainty in regional climate change projections. *Bulletin of the American Meteorological Society*, 99, 2093–2106.

Karmalkar, A.V., Thibeault, J.M., Bryan, A.M. and Seth, A. (2019) Identifying credible and diverse GCMs for regional climate change studies—case study: northeastern United States. *Climatic Change*, 154, 367–386.

Kelley, M., Schmidt, G.A., Nazarenko, L.S., Bauer, S.E., Ruedy, R., Russell, G.L., Ackerman, A.S., Aleinov, I., Bauer, M., Bleck, R., Canuto, V., Cesana, G., Cheng, Y., Clune, T.L., Cook, B.I., Cruz, C.A., Del Genio, A.D., Elsaesser, G.S., Faluvegi, G., Kiang, N.Y., Kim, D., Lacis, A.A., Leboissetier, A., LeGrande, A. N., Lo, K.K., Marshall, J., Matthews, E.E., McDermid, S., Mezuman, K., Miller, R.L., Murray, L.T., Oinas, V., Orbe, C., García-Pando, C.P., Perlwitz, J.P., Puma, M.J., Rind, D., Romanou, A., Shindell, D.T., Sun, S., Tausnev, N., Tsigaridis, K., Tselioudis, G., Weng, E., Wu, J. and Yao, M.S. (2020) GISS-E2.1: configurations and climatology. *Journal of Advances in Modeling Earth Systems*, 12, e2019MS002025.

Knutti, R. (2010) The end of model democracy? *Climatic Change*, 102, 395–404.

Lanzante, J.R., Dixon, K.W., Nath, M.J., Whitlock, C.E. and Adams-Smith, D. (2018) Some pitfalls in statistical downscaling of future climate. *Bulletin of the American Meteorological Society*, 99, 791–803.

Leduc, M., Laprise, R., de Elia, R. and Separovic, L. (2016) Is institutional democracy a good proxy for model independence? *Journal of Climate*, 29, 8301–8316.

Lee, J.Y., Marotzke, J., Bala, G., Cao, L., Corti, S., Dunne, J.P., Engelbrecht, F., Fischer, E., Fyfe, J.C., Jones, C., Maycock, A., Mutemi, J., Ndiaye, O., Panickal, S. and Zhou, T. (2021) Future global climate: scenario-based projections and near-term information. In: Masson-Delmotte, V., Zhai, P., Pirani, A., Connors, S.L., Péan, C., Berger, S., Caud, N., Chen, Y., Goldfarb, L., Gomis, M.I., Huang, M., Leitzell, K., Lonnoy, E., Matthews, J.B.R., Maycock, T.K., Waterfield, T., Yelekçi, O., Yu, R. and Zhou, B. (Eds.) *Climate Change 2021: The Physical Science Basis. Contribution of Working Group I to the Sixth Assessment Report of the Intergovernmental Panel on Climate Change*. Cambridge and New York, NY: Cambridge University Press, pp. 1–195.

Liang, Y., Gillett, N.P. and Monahan, A.H. (2020) Climate model projections of 21st century global warming constrained using the observed warming trend. *Geophysical Research Letters*, 47, 1–10.

Lindvall, J. and Svensson, G. (2015) The diurnal temperature range in the CMIP5 models. *Climate Dynamics*, 44, 405–421.

Maraun, D. (2016) Bias correcting climate change simulations—a critical review. *Current Climate Change Reports*, 2, 211–220.

McSweeney, C.F., Jones, R.G., Lee, R.W. and Rowell, D.P. (2014) Selecting CMIP5 GCMs for downscaling over multiple regions. *Climate Dynamics*, 44, 3237–3260.

Meehl, G.A., Senior, C.A., Eyring, V., Flato, G., Lamarque, J.F., Stouffer, R.J., Taylor, K.E. and Schlund, M. (2020) Context for interpreting equilibrium climate sensitivity and transient climate response from the CMIP6 Earth system models. *Science Advances*, 6, 1–11.

Milinski, S., Maher, N. and Olonscheck, D. (2019) How large does a large ensemble need to be? *Earth System Dynamics, Discussions*, 11, 885–901.

Minder, J.R., Letcher, T.W. and Liu, C. (2018) The character and causes of elevation-dependent warming in high-resolution simulations of Rocky Mountain climate change. *Journal of Climate*, 31, 2093–2113.

Müller, W.A., Jungclaus, J.H., Mauritsen, T., Baehr, J., Bittner, M., Budich, R., Bunzel, F., Esch, M., Ghosh, R., Haak, H., Ilyina, T., Kleine, T., Kornblueh, L., Li, H., Modali, K., Notz, D., Pohlmann, H., Roeckner, E., Stemmler, I., Tian, F. and Marotzke, J. (2018) A higher-resolution version of the Max Planck Institute earth system model (MPI-ESM1.2-HR). *Journal of Advances in Modeling Earth Systems*, 10, 1383–1413.

O'Neill, B.C., Tebaldi, C., Van Vuuren, D.P., Eyring, V., Friedlingstein, P., Hurtt, G., Knutti, R., Kriegler, E., Lamarque, J.F., Lowe, J., Meehl, G.A., Moss, R., Riahi, K. and Sanderson, B.M. (2016) The scenario model intercomparison project (ScenarioMIP) for CMIP6. *Geoscientific Model Development*, 9, 3461–3482.

Palazzi, E., Mortarini, L., Terzago, S. and von Hardenberg, J. (2019) Elevation-dependent warming in global climate model simulations at high spatial resolution. *Climate Dynamics*, 52, 2685–2702.

Pepin, N., Bradley, R.S., Diaz, H.F., Baraer, M., Caceres, E.B., Forsythe, N., Fowler, H., Greenwood, G., Hashmi, M.Z., Liu, X. D., Miller, J.R., Ning, L., Ohmura, A., Palazzi, E., Rangwala, I., Schöner, W., Severskiy, I., Shahgedanova, M., Wang, M.B., Williamson, S.N. and Yang, D.Q. (2015) Elevation-dependent warming in mountain regions of the world. *Nature Climate Change*, 5, 424–430.

Pierce, D.W., Barnett, T.P., Santer, B.D. and Gleckler, P.J. (2009) Selecting global climate models for regional climate change studies. *Proceedings of the National Academy of Sciences of the United States of America*, 106, 8441–8446.

Ribes, A., Qasmi, S. and Gillett, N.P. (2021) Making climate projections conditional on historical observations. *Science Advances*, 7, 1–10.

Rupp, D.E., Abatzoglou, J.T., Hegewisch, K.C. and Mote, P.W. (2013) Evaluation of CMIP5 20th century climate simulations for the Pacific Northwest USA. *Journal of Geophysical Research: Atmospheres*, 118, 10884–10906.

Salathé, E.P., Steed, R., Mass, C.F. and Zahn, P.H. (2008) A high-resolution climate model for the U.S. Pacific northwest: meso-scale feedbacks and local responses to climate change. *Journal of Climate*, 21, 5708–5726.

Schlund, M., Lauer, A., Gentine, P., Sherwood, S.C. and Eyring, V. (2020) Emergent constraints on equilibrium climate sensitivity in CMIP5: Do they hold for CMIP6? *Earth System Dynamics*, 11, 1233–1258.

Schmidt, G.A. (2021) #NotAllModels. RealClimate. Available at: https://www.realclimate.org/index.php/archives/2021/08/notallmodels/ [Accessed 4th January 2022].

Séférian, R., Nabat, P., Michou, M., Saint-Martin, D., Voldoire, A., Colin, J., Decharme, B., Delire, C., Berthet, S., Chevallier, M., Sénési, S., Franchisteguy, L., Vial, J., Mallet, M., Joetzjer, E., Geoffroy, O., Guérémy, J.F., Moine, M.P., Msadek, R.,

Ribes, A., Rocher, M., Roehrig, R., Salas-y-Mélia, D., Sanchez, E., Terray, L., Valcke, S., Waldman, R., Aumont, O., Bopp, L., Deshayes, J., Éthé, C. and Madec, G. (2019) Evaluation of CNRM earth system model, CNRM-ESM2-1: role of earth system processes in present-day and future climate. *Journal of Advances in Modeling Earth Systems*, 11, 4182–4227.

Sellar, A.A., Jones, C.G., Mulcahy, J.P., Tang, Y., Yool, A., Wiltshire, A., O'Connor, F.M., Stringer, M., Hill, R., Palmieri, J., Woodward, S., de Mora, L., Kuhlbrodt, T., Rumbold, S.T., Kelley, D.I., Ellis, R., Johnson, C.E., Walton, J., Abraham, N.L., Andrews, M.B., Andrews, T., Archibald, A.T., Berthou, S., Burke, E., Blockley, E., Carslaw, K., Dalvi, M., Edwards, J., Folberth, G.A., Gedney, N., Griffiths, P.T., Harper, A.B., Hendry, M.A., Hewitt, A.J., Johnson, B., Jones, A., Jones, C.D., Keeble, J., Liddicoat, S., Morgenstern, O., Parker, R.J., Predoi, V., Robertson, E., Siahaan, A., Smith, R.S., Swaminathan, R., Woodhouse, M.T., Zeng, G. and Zerroukat, M. (2019) UKESM1: description and evaluation of the U.K. earth system model. *Journal of Advances in Modeling Earth Systems*, 11, 4513–4558.

Sherwood, S., Webb, M.J., Annan, J.D., Armour, K.C., Forster, P. M., Hargreaves, J.C., Hegerl, G., Klein, S.A., Marvel, K.D., Rohling, E.J., Watanabe, M., Andrews, T., Braconnot, P., Bretherton, C.S., Foster, G.L., Hausfather, Z., von der Heydt, A. S., Knutti, R., Mauritsen, T., Norris, J.R., Proistosescu, C., Rugenstein, M., Schmidt, G.A., Tokarska, K.B. and Zelinka, M. D. (2020) An assessment of Earth's climate sensitivity using multiple lines of evidence. *Reviews of Geophysics*, 58, e2019RG000678.

Sutton, R.T. (2018) ESD ideas: a simple proposal to improve the contribution of IPCC WGI to the assessment and communication of climate change risks. *Earth System Dynamics*, 9, 1155–1158.

Sutton, R.T. and Hawkins, E. (2020) ESD ideas: global climate response scenarios for IPCC assessments. *Earth System Dynamics*, 11, 751–754.

Swart, N.C., Cole, J.N.S., Kharin, V.V., Lazare, M., Scinocca, J.F., Gillett, N.P., Anstey, J., Arora, V., Christian, J.R., Hanna, S., Jiao, Y., Lee, W.G., Majaess, F., Saenko, O.A., Seiler, C., Seinen, C., Shao, A., Sigmond, M., Solheim, L., Von Salzen, K., Yang, D. and Winter, B. (2019) The Canadian Earth System Model version 5 (CanESM5.0.3). *Geoscientific Model Development*, 12, 4823–4873.

Tabor, K. and Williams, J.W. (2010) Globally downscaled climate projections for assessing the conservation impacts of climate change. *Ecological Applications*, 20, 554–565.

Tatebe, H., Ogura, T., Nitta, T., Komuro, Y., Ogochi, K., Takemura, T., Sudo, K., Sekiguchi, M., Abe, M., Saito, F., Chikira, M., Watanabe, S., Mori, M., Hirota, N., Kawatani, Y., Mochizuki, T., Yoshimura, K., Takata, K., O'ishi, R., Yamazaki, D., Suzuki, T., Kurogi, M., Kataoka, T., Watanabe, M. and Kimoto, M. (2018) Description and basic evaluation of simulated mean state, internal variability, and climate sensitivity in MIROC6. *Geoscientific Model Development*, 12, 2727–2765.

Taylor, K.E., Stouffer, R.J. and Meehl, G.A. (2012) An overview of CMIP5 and the experiment design. *Bulletin of the American Meteorological Society*, 93, 485–498.

Volodin, E.M., Mortikov, E.V., Kostrykin, S.V., Galin, V.Y., Lykossov, V.N., Gritsun, A.S., Diansky, N.A., Gusev, A.V. and Iakovlev, N.G. (2017) Simulation of the present-day climate with the climate model INMCM5. *Climate Dynamics*, 49, 3715–3734.

Wang, K. and Clow, G.D. (2020) The diurnal temperature range in CMIP6 models: climatology, variability, and evolution. *Journal of Climate*, 33, 8261–8279.

Wang, T., Hamann, A., Spittlehouse, D. and Carroll, C. (2016) Locally downscaled and spatially customizable climate data for historical and future periods for North America. *PLoS One*, 11, e0156720.

Wang, T., Hamann, A., Spittlehouse, D.L. and Murdock, T.Q. (2012) ClimateWNA: high-resolution spatial climate data for western North America. *Journal of Applied Meteorology and Climatology*, 51, 16–29.

Wilby, R.L., Charles, S.P., Zorita, E., Timbal, B., Whetton, P. and Mearns, L.O. (2004) *Guidelines for Use of Climate Scenarios Developed from Statistical Downscaling Methods. IPCC Task Group on Data and Scenario Support for Impact and Climate Analysis (TGICA)*. Geneva: IPCC.

Wilson, L.J., Vallee, M. and Montpetit, J. (2008) Comments on "Hydrometeorological accuracy enhancement via post-processing of numerical weather forecasts in complex terrain". *Weather and Forecasting*, 24, 892–894.

Wu, T., Lu, Y., Fang, Y., Xin, X., Li, L., Li, W., Jie, W., Zhang, J., Liu, Y., Zhang, L., Zhang, F., Zhang, Y., Wu, F., Li, J., Chu, M., Wang, Z., Shi, X., Liu, X., Wei, M., Huang, A., Zhang, Y. and Liu, X. (2019) The Beijing Climate Center Climate System Model (BCC-CSM): the main progress from CMIP5 to CMIP6. *Geoscientific Model Development*, 12, 1573–1600.

Yukimoto, S., Kawai, H., Koshiro, T., Oshima, N., Yoshida, K., Urakawa, S., Tsujino, H., Deushi, M., Tanaka, T., Hosaka, M., Yabu, S., Yoshimura, H., Shindo, E., Mizuta, R., Obata, A., Adachi, Y. and Ishii, M. (2019) The meteorological research institute Earth system model version 2.0, MRI-ESM2.0: description and basic evaluation of the physical component. *Journal of the Meteorological Society of Japan*, 97, 931–965.

Ziehn, T., Chamberlain, M.A., Law, R.M., Lenton, A., Bodman, R. W., Dix, M., Stevens, L., Wang, Y.P. and Srbinovsky, J. (2020) The Australian Earth System Model: ACCESS-ESM1.5. *Journal of Southern Hemisphere Earth Systems Science*, 70, 193–214.